

## Cosmic Ray Electron Synchrotron Telescope (CREST) status report

S. NUTTER<sup>1</sup>, C. R. BOWER<sup>2</sup>, S. COUTU<sup>3</sup>, J. GENNARO<sup>4</sup>, M. GESKE<sup>3</sup>, D. MÜLLER<sup>5</sup>, J. MUSSER<sup>2</sup>, N. H. PARK<sup>5</sup>, M. SCHUBNELL<sup>4</sup>, G. TARLÉ<sup>4</sup>, AND S. P. WAKELY<sup>5</sup>.

<sup>1</sup> Northern Kentucky University, Highland Heights, KY 41099 USA

<sup>2</sup> Indiana University, Bloomington, IN 47405 USA

<sup>3</sup> Pennsylvania State University, University Park, PA 16802 USA

<sup>4</sup> University of Michigan, Ann Arbor, MI 48109 USA

<sup>5</sup> University of Chicago, Chicago, IL 60637 USA

nutters@nku.edu

**Abstract:** The CREST instrument aims to detect cosmic electrons beyond a few TeV, which would likely originate in the local Galactic neighborhood, within a kpc or so, owing to their rapid energy loss rates during propagation. Only a few candidate acceleration sites exist within this horizon, such as Vela, Monogem, and the Cygnus Loop remnants, and thus multi-TeV electrons are a useful marker of the nearby high energy universe. CREST detects electrons through their geosynchrotron x-ray emissions in the South polar regions of the Earth. The signature is a stream of x-ray photons emitted in the plane of electron travel, intersecting the plane of a horizontal detector array; the net effect is a co-linear arrangement of x-ray hits coincident in time. To this end an array of 1024 BaF<sub>2</sub> crystal detectors was built, surrounded by veto plastic scintillators to guard against chance alignments of charged particles in air showers. This instrument was successfully flown on a high-altitude balloon for 10 days in Antarctica, starting December 25, 2011, and recovered in February 2012. The status of the analysis of the data from this flight is presented.

**Keywords:** cosmic rays, electrons, geosynchrotron radiation, balloons.

### 1 Introduction

Electrons of energy above a few TeV are a largely unexplored component of the cosmic-ray flux at the Earth despite strong evidence of their presence in a number of supernova remnants (e.g., SN 1006). The detection of such electrons at Earth would be extremely significant, yielding information about the spatial distribution of nearby cosmic-ray sources. Electrons lose energy rapidly as they propagate through the Galaxy due to synchrotron losses in the galactic magnetic fields and inverse Compton interactions with the cosmic microwave background radiation. These losses are so severe that a 1 TeV electron observed at the Earth is expected to have originated within a distance of less than 1 kpc. If high-energy cosmic-ray electrons originate in supernova shock acceleration processes, as is the current paradigm for cosmic rays in general [1], there would be few known supernova remnants within this horizon from which these particles could originate. The spectral shape of high-energy electrons should, therefore, be strongly affected by the number of nearby sources, and their space-time distribution. Indeed, the absence of any such features in the high-energy electron spectrum, whether they be cut-offs or upturns from sources, would be unexpected and would call into question our understanding of cosmic-ray sources and propagation.

Current and past dedicated electron detectors, typically flown by high altitude balloons, have been limited in their ability to study the highest energy cosmic-ray electrons by their short exposure times and small apertures. Recently, ground and space-based gamma-ray instruments have made impressive strides in the study of ultra-high energy electrons [3][4][5], but even these large acceptance/long exposure instruments have not provided measurements above

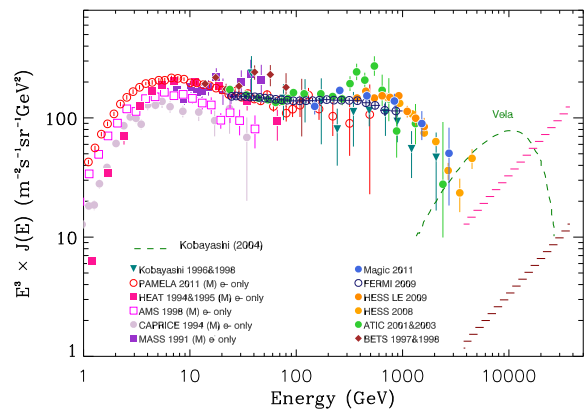


**Fig. 1:** All-electron energy spectrum measurements to date. The UHE flux from Vela predicted by one set of model parameters, described in [2], is shown as a dashed line. The top hatched line shows the anticipated CREST sensitivity for the recently completed 10 day flight, while the bottom hatched line shows that for a 50 day flight.

electron energies of a few TeV. Moreover, the ground-based techniques cannot distinguish a signal from a cosmic electron from that from a cosmic gamma ray. The CREST instrument has adopted a radically different approach to the detection of electrons of energies between 2 and 50 TeV, using a novel technique for the identification of high energy electrons proposed and developed by a number of workers over the years [6] [7]. CREST employs an array of BaF<sub>2</sub> scintillation detectors to observe the synchrotron photons

generated at x-ray and gamma-ray energies by these electrons in the Earth's magnetic field. These photons will be coincident in time and highly co-linear in the scintillator array, yielding a clear signal signature. This technique results in a substantial increase in the acceptance and sensitivity of the apparatus relative to its physical size.

## 2 Detector Overview

The CREST detector concept is presented in Figure 2. Detection of the primary electron is achieved through the observation of its synchrotron radiation, resulting in large effective detector apertures since the instrument needs only to intersect just a portion of the line of photons and not necessarily the trajectory of the electron itself. The effective area of the detector is determined by the dimension  $R_s$  convolved with the physical size of the detector.

To separate synchrotron-induced events from background photons, two characteristics of the radiation must be exploited - the formation of a line of photons at the detector and the very short time interval over which these photons are deposited. This is accomplished in the CREST instrument by using a spatially segmented detector with nanosecond timing resolution.

To efficiently detect photons in the hard x-ray range a high-Z detector material is required. The CREST detector employs an array of inorganic scintillator detectors combined with photomultiplier tube (PMT) readout. This combination provides sensitivity over the entire photon energy range of interest, from the  $>10$  MeV photons produced by the highest energy electrons down to photon energies of 40 keV, below which atmospheric absorption strongly attenuates the photon flux. Barium Fluoride ( $\text{BaF}_2$ ) is used as the active detector in the CREST instrument because of its relatively high density and light yield, and because of its fast scintillation component, which provides timing resolution of roughly 1 ns. An array of 1024 of these crystals, each with a thickness of 2 cm and a diameter of 5 cm is used.

As shown in Figure 2, the crystal array is arranged in a rectangular pattern. The detectors are placed on a grid with a uniform  $7.5 \text{ cm} \times 7.5 \text{ cm}$  spacing, covering a total area of roughly  $2.4 \times 2.4 \text{ m}^2$ . Each crystal is surrounded by a 0.4 cm thick lead shield which reduces the rate of multiple crystal hits resulting from Compton scatters of single incident x-rays in the support frame and other material below the array. The crystal array is grouped in blocks of 16 which share a common front-end readout board set. The PMTs in each of these blocks are supported within a  $0.14 \text{ g/cm}^3$  matrix of polyethylene foam. Groups of 8 of

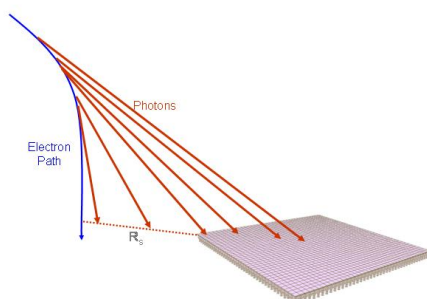


Fig. 2: CREST electron detection concept.

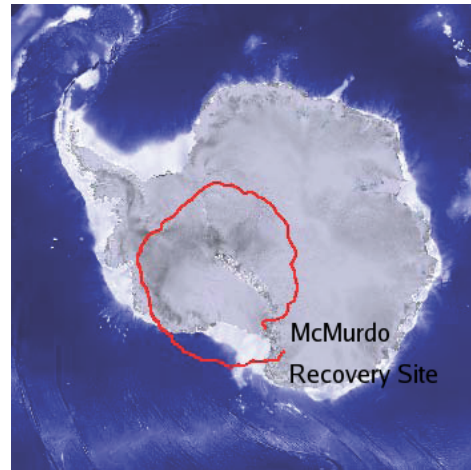


Fig. 3: CREST Flight 629N Trajectory, December 25, 2011 - January 5, 2012.

these blocks in a row share a common mechanical support channel, facilitating recovery and shipping.

The crystal array is surrounded on all sides by a 0.5 cm thick plastic scintillator veto shield which provides rejection against the copious flux of charged particles.

## 3 Flight Overview

The first long-duration balloon (LDB) flight of the CREST instrument took place during the 2011/2012 Antarctic season, with launch on December 25, 2011, and termination on January 5, 2012. Figure 3 shows the orbital trajectory of the instrument over the flight, which was terminated after one circumpolar orbit. The decision to terminate after one orbit was motivated by concern that a second orbit would have, most likely, led to a difficult and late recovery of the instrument. The detector performed well throughout the flight, collecting over  $4 \times 10^9$  minimum bias events during the 10 days at float.

Figure 4 shows the atmospheric pressure measured at the instrument as a function of time during the flight. This is a particularly important parameter for CREST, as the effective area of the instrument is dependent upon the atmospheric overburden due to its absorbing effect on synchrotron photons in transit. Clearly, flying higher is better - and hence future CREST flights would attempt to

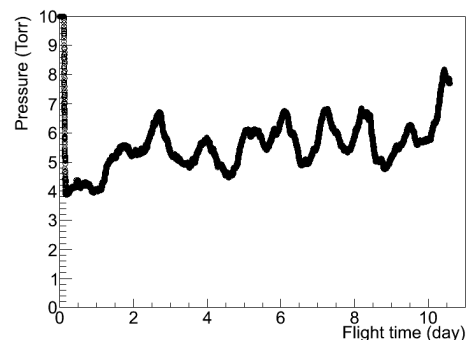
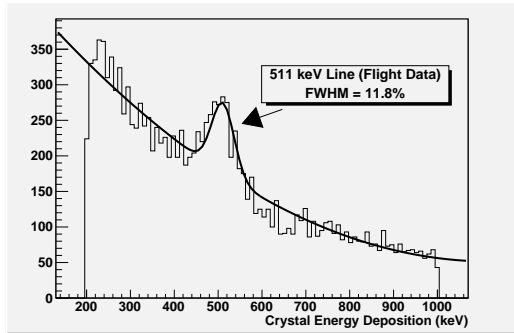


Fig. 4: Flight pressure profile.



**Fig. 5:** Fit to the 511 keV annihilation line observed in flight.

utilize lighter payloads to enable the use of higher-altitude balloons.

#### 4 Instrument Performance

The steeply falling cosmic-ray electron energy spectrum necessitates a well understood and characterized detector energy response as well as the minimization of systematic errors. The energy deposition in a crystal is measured with a single bit resolution of 1 keV, and with a full scale of roughly 50 MeV. The energy scale is calibrated as a function of time during the flight using the 511 keV annihilation line, as well as a number of alpha decays with energies between 1.3 and 2.6 MeV resulting from trace radioactive contaminants in the BaF<sub>2</sub> crystal. Figure 5 contains a typical fit to the 511 keV annihilation line during flight. The timing resolution of the crystal array is a critical parameter, as it determines the rejection power of the instrument to backgrounds due to the random coincidence of multiple events. The timing measurements in the BaF<sub>2</sub> detectors and veto paddles are based on a common system clock operating at 1 GHz, and therefore the scale factor relating the digitized time measurement to true time is a global system parameter determined by the system clock frequency alone. Calibration of the instrument timing system consists in the determination of channel to channel timing offsets, along with time-walk corrections. After calibration, a timing resolution for flight data of better than 1 ns is achieved. The timing response of the instrument seen during flight is

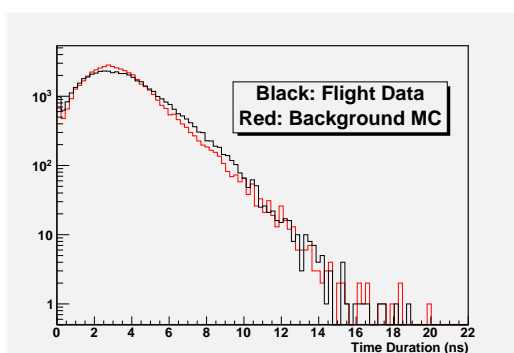


**Fig. 6:** Event duration, in nanoseconds. The black histogram represents flight data, while the red histogram represents the Monte Carlo prediction of this distribution.

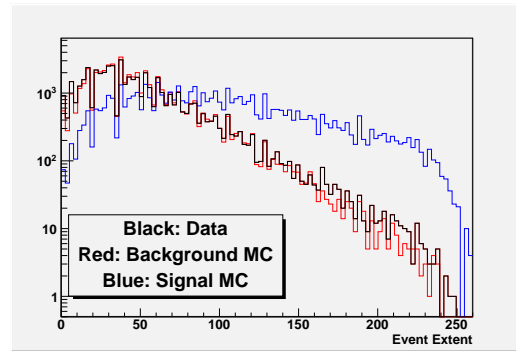


**Fig. 7:** Event spatial extent along the principal axis, in cm.

well characterized by the Monte Carlo detector response simulation, as shown in Figure 6.

In the CREST data set we are searching for rare electron-induced events in a sea of potential backgrounds, and therefore the modeling of these backgrounds is of particular importance. For this purpose, we adopt the GLAST/Fermi atmospheric flux model, which includes both upward and downward going flux components [9]. A significant component to the analysis effort to date has been verifying that the instrument model accurately describes the flight data. An example is depicted in Figure 7, which shows a comparison between the reconstructed event spatial extent in the crystal array along its principal axis for flight data, shown in black, simulated background events shown in red, and for simulated electron events in blue. This figure is representative of the excellent agreement we obtain between the instrument response seen in the flight data and the simulated response. This simulation validation effort is now largely completed, with production of a large volume of simulated data sets currently in progress.

#### 5 Analysis Status

As discussed above, the instrumental signature of a 'golden' synchrotron event from a high-energy electron is a set of co-linear, isochronous crystal hits. An example of such an event from the flight data is shown in Figure 8. Signal events are selected primarily on the basis of the level of activity (or lack thereof) in the veto system and the co-linearity of hits in the crystal array. The analysis of crystal event data begins with a clustering algorithm that seeks to combine neighboring crystal hits resulting from a single incident gamma ray into a single cluster. The spatial and temporal locations of these clusters are then used in a search for linear, isochronous signal events. In Figure 9 we present the  $1/v$  distribution of events in the flight data which satisfy the criteria described below, where  $v$  is the propagation velocity of the event in the crystal array along its major axis. Here, cluster positions are measured in a given event with respect to the cluster centroid furthest from the array center. Shown are all events from the flight with no veto activity, greater than 4 crystal hit clusters, an event extent in the crystal array of at least 50 cm, and a reduced  $\chi^2$  value of the fit to the  $x$  vs  $y$  crystal cluster centroid position of less than 5. The two peaks seen in this figure correspond to propagation in either direction along the major axis of the event. The fit shown in this figure illustrates that this dataset can be well described by two Gaussian distributions centered at  $1/v = \pm 1/c$ , indicative of a signal source propagating across the detector

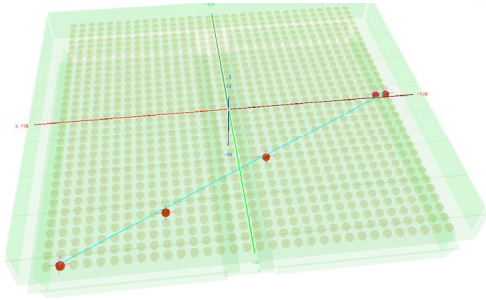


**Fig. 8:** Event display of signal-like event from the LDB flight.

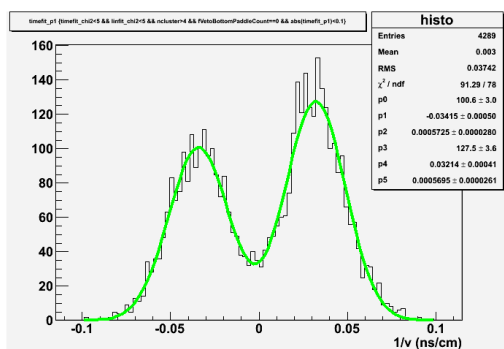


**Fig. 9:** Inverse event propagation speed for selected flight data.

at the speed of light (for example, due to a single charged particle missed by the veto system, or a linear chain of causally connected gamma-ray interactions). The signal we seek does not exhibit this behavior, since the synchrotron-induced photons propagate on a common wave front that is perpendicular to the local magnetic field direction. In the case of a vertical magnetic field the synchrotron photons arrive at the detector at the same instant, independent of the angle of incidence of the primary electron. Such a signal would be seen as an excess in events near  $1/v=0$  in Figure 9. Figure 10 demonstrates this, showing for the same set of data selections the  $1/v$  distribution predicted for synchrotron events at the magnetic field inclination seen at McMurdo. A central thrust of our future data analysis efforts will be optimizing our sensitivity to the signal represented in Figure 10 within the distribution shown in Figure 9.

A significant analysis task that remains to be carried out in our analysis program is a careful accounting of the effect of the payload's varying geomagnetic location and atmospheric depth on signal and background rates during the flight. Since the production of synchrotron photons and their relative time of arrival at the detector are dependent on the direction of the Earth's magnetic field, a careful modelling of the field configuration along the flight path will be important. As mentioned earlier, we are in the process of producing a large volume simulation of the instrument's response to all relevant backgrounds, allowing data distributions such as show in Figure 9 to be compared with Monte Carlo data samples of equivalent or greater statistics. Optimization of the data selections used, and a refined understanding of the relationship between total synchrotron and bremsstrahlung activity observed in

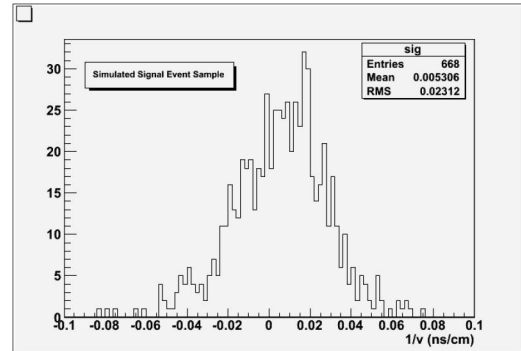


**Fig. 10:** Simulated signal event inverse propagation speed.

CREST to the energy of the primary electron are other areas of intense effort.

## 6 Conclusions

Figure 1 shows the expected sensitivity of CREST for the 10 day flight just completed, and for a 50 day total exposure, which should be easily achievable under a program of future re-flights.

With the analysis now underway, we expect to demonstrate the efficacy of the geosynchrotron detection technique. With another, longer, flight, a lighter CREST instrument has the potential to detect electrons at extremely high energies, beyond the range of planned instruments such as CALET, and competitive with air shower instruments, but without the gamma and proton background that affects electron measurements with that technique.

**Acknowledgments:** This work has been supported under NASA Grants NNX08AC42G, NNX08AC40G, NNX08AD08G, and NNG04WC34G, and the Kentucky Space Grant. We would like to thank the Columbia Scientific Balloon Facility and the CSBF launch crews for their excellent support of balloon missions. The collaboration also gratefully acknowledges the contributions of T. Anderson, J. Ameel, J. Bench, T. Bishay, M. Gebhard, B. Kunkler, B. Martin, R. Northrop, A. Shroyer, C. Smith, and K. Wallace.

## References

- [1] M. Ackermann *et al.*, Science 339,807 (2013).
- [2] T. Kobayashi *et al.*, ApJ 601, 340 (2004).
- [3] Aguilar *et al.*, Phys Lett. B bf646 145 (2007).
- [4] M. Ackermann *et al.*, Phys. Rev. Lett. 108, 1 (2012).
- [5] O. Adriani *et al.*, Nature 458, 7238 (2009).
- [6] O.F. Prilutskiy, ZhETF 19, 320 (1972).
- [7] S.A. Stephens & V.K. Balasubrahmanyam J. Geophys. Res. 88, A10 (1983).
- [8] M. Schönberg and S. Chandrasekhar, The Astrophysical Journal 96 (1942) 161-172 doi:10.1086/144444.
- [9] T. Mizuno *et al.*, ApJ 614,1113 (2004).